"Layer-Filter Threshold" Technique for Near-Infrared Laser Ablation in Organic Semiconductor Device Processing

*Feng Ye, Zhaobin Chen, Xiaoli Zhao, Jiayue Chen, and Xiaoniu Yang**

Although conventional laser ablation (CLA) method has widely been used in patterning of organic semiconductor thin films, its quality control still remains unsatisfied due to the ambiguous photochemical and photothermal processes. Based on industrial available near-infrared laser source, herein, a novel "layer-filter threshold" (LFT) technique is proposed, which involves the decomposition of targeted "layer-filter" and subsequent explosive evaporation process to purge away the upper layers instead of layer-by-layer ablation. For photovoltaic device with structure of metal/blend/PEDOT:PSS/ITO/glass, the PEDOT:PSS layer as the "layer-filter" is first demonstrated to be effective, and then the merged P1–P2 line and metal electrode layer are readily patterned through the "self-aligned" effect and regulation of ablation direction, respectively. The correlation between laser fluence and explosive ablation efficacy is also investigated. Finally, photovoltaic modules based on classical P3HT:$PC_{61}BM$ and low-bandgap PBDT-TFQ:$PC_{71}BM$ systems are separately fabricated following the LFT technique. It is found that over 90% of geometric fill factor is achieved while device performances maintain in a limited change with increased number of series cells. In comparison to conventional laser ablation methods, the LFT technique does not require sophisticated instruments but reaches comparable processing accuracy, which shows promising potential in the fabrication and commercialization of organic semiconductor thin-film devices.

1. Introduction

Organic semiconductors have been seen as potential alternatives to the traditional inorganic materials due to their flexibility and solution-processed compatibility, and thus provide the room for application diversification and processing cost reduction.[1–7] In the large-scale production of organic electronic devices, an efficient patterning method with satisfactory precision is critical to a controllable material consumption and the improvement in device performance.[8–11] So far, the techniques for creating patterned films such as inkjet, screen, flexography, and gravure printing have been proved to possess broad application for their high throughput and roll-to-roll compatibility.[12–14] While the laser ablation technique as a postpatterning method for the fully coated films provides another possibility for the mass production of patterned organic multilayers and gets point for its high potential in miniaturization.[15–17]

In the fabrication of multilayer thin film devices, the challenge vital to the refinement of the structure is to achieve the complete removal of specific layers in a certain microregion pattern while avoiding damage to adjacent layers. Conventional laser ablation (CLA) method is based on the photochemical and photothermal mechanisms.[18,19] In order to achieve the controllable ablation depth and also to eliminate the attendant carbonation raised bulges caused by the irradiation damage of the materials, ultrafast laser ablation with pulse duration of femtosecond or picosecond is commonly preferred for its highly concentrated energy and the inhibitory of thermal diffusion process.[20,21] However, for CLA method, which involves the layer-by-layer ablation from the top to the bottom of the multilayer structure, a fine adjustment of the laser instrument is needed, and most important, in common cases, only one instrument may not satisfy the requirements, due to the differentiated sensitivity of materials with various layer sequence and film thickness.[22] These disadvantages limit the application of the laser ablation in organic multilayer devices.

In addition to the pulse duration, it is well known that the ablation is also influenced by the laser wavelength and the fluence.[23,24] As a practical case, in the study on large area polymer solar cell (PSC) module devices of this group, it is found that the layers made of different materials show different sensitivity to the laser wavelength and the energy-related parameters. Through ablating the particular interlayer by laser irradiation, one could realize the complete removal of the cover layers under the confined explosive evaporation, without imparting

F. Ye, Dr. X. Zhao, J. Chen, Prof. X. Yang
State Key Laboratory of Polymer Physics and Chemistry
Changchun Institute of Applied Chemistry
Chinese Academy of Sciences
5625 Renmin Street, Changchun 130022, P. R. China
E-mail: xnyang@ciac.jl.cn
F. Ye, Prof. Z. Chen, Dr. X. Zhao, J. Chen, Prof. X. Yang
Polymer Composites Engineering Laboratory
Changchun Institute of Applied Chemistry
Chinese Academy of Sciences
5625 Renmin Street, Changchun 130022, P. R. China
F. Ye, J. Chen
University of Chinese Academy of Sciences
Beijing 100049, P. R. China

DOI: 10.1002/adfm.201501688

the effects on adjacent bottom layers. This provides us with a smart chance to develop a new patterning method for multilayer devices.

In this study, a novel strategy, here we called "layer-filter threshold" (LFT) technique, is developed. The rationale of the LFT method is first demonstrated, and then used to fabricate the photovoltaic module device based on poly(3-hexylthiophene) (P3HT) and [6,6]-phenyl-C_{61}-butyric acid methyl ester ($PC_{61}BM$) blend film with the layer sequence of Al/Ca/blend/PEDOT:PSS/ITO/glass. For the near-infrared (NIR) laser instrument with 1064 nm of wavelength, the PEDOT:PSS layer could serve as the "layer-filter", the confined pressure environment is then constructed under irradiation, which is sufficient to initiate the explosive evaporation process and therefore realizes the complete removal of the cover layers (active layer, top electrode layer). The LFT technique is further verified to be applicable for the low-bandgap material system of poly{4,8-bis(2′-ethylhexyloxy)-benzo[1,2-b:4,5-b′]-dithiophene-alt-[5,8-bis(5′-thiophen-2′-yl)-6,7-difluoro-2,3-bis-(3″-hexyloxyphenyl)-quinoxaline]} (PBDT-TFQ): [6,6]-phenyl-C_{71}-butyric acid methyl ester ($PC_{71}BM$).

2. Results and Discussion

2.1. LFT Technique

According to the LFT technique, instead of vaporizing the target materials layer by layer with split-second highly focused energy, a confined pressure environment is constructed in the built-in "layer-filter" by irradiation. This pressure is sufficient to initiate the explosive evaporation process and thus purge away the layers covered on the top of the "layer-filter".

The first important point for LFT technique is the identification of the "layer-filter," which is expected to be the most sensitive layer to irradiation heating and thus could initiate the split of the cover layers through underlying explosive evaporation process. The thermogravimetric analysis (TGA) curves shown in **Figure 1**a reveals that the decomposition temperature for 5% weight loss is 250 °C for PEDOT:PSS, which is much lower than that for P3HT (447 °C) and $PC_{61}BM$ (417 °C). In other words, the PEDOT:PSS layer in multilayer structure is appropriate to serve as the "layer-filter" for LFT technique.

As mentioned above, different materials possess different resistance to the laser ablation under certain conditions. In order to achieve the targeted vaporization of PEDOT:PSS "layer-filter", a specific wavelength must be selected so that the hierarchical differentiated photothermal conversion could proceed in the multilayer structure without any significant thermal impact on the other layers. Figure 1b shows the UV–vis absorption spectra of PEDOT:PSS, P3HT:$PC_{61}BM$, and ITO, which are normalized by the film thickness and show that the absorbance of PEDOT:PSS film is roughly an order of magnitude higher than that of P3HT:$PC_{61}BM$ and ITO around the 1000 nm of wavelength. In other words, the laser with the wavelength in this range almost does not bring the photothermal effect on P3HT:$PC_{61}BM$ and ITO. Therefore, 1064 nm wavelength in the NIR region is selected in this study due to its wide industrial availability. It is noteworthy that this is different from previous works, in which 520 nm wavelength in visible region was reported for organic layer ablation[15,16,25,26] while the 1064 nm was not recommended due to the elusive process window for clear ablation and the terrible edge bulge of up to hundreds of nanometers.[27,28] The reason for this departure is mainly due to the different ablation mechanisms between the conventional

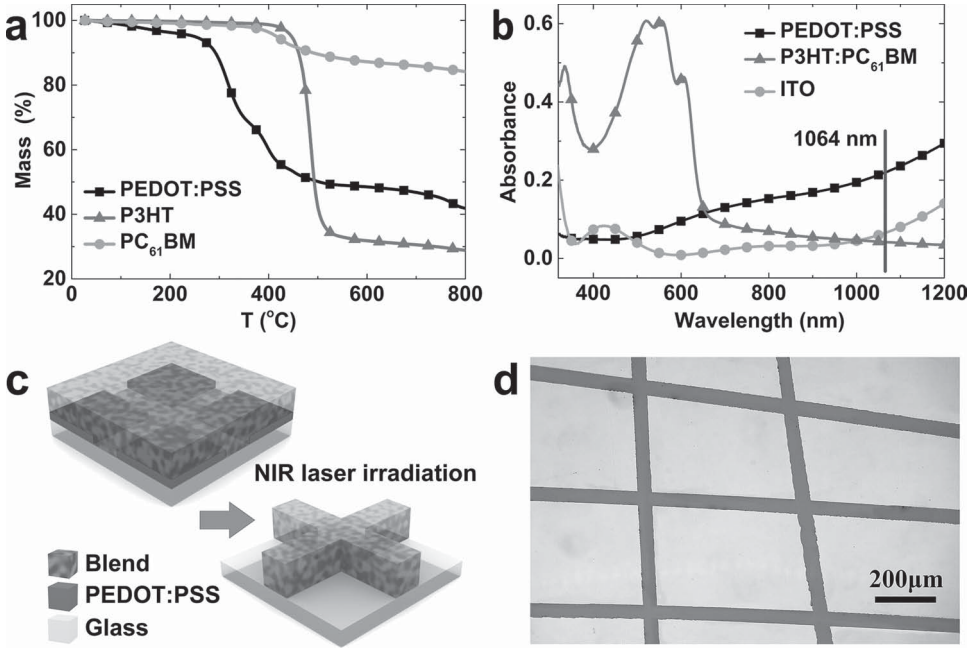

Figure 1. a) TGA thermograms of PEDOT:PSS, P3HT, and $PC_{61}BM$. b) Film absorption spectra of PEDOT:PSS, P3HT:$PC_{61}BM$ blend, and ITO. Blue vertical line indicates the position of 1064 nm wavelength. c) Demo scheme of LFT process. d) OM image of the mesh pattern processed by LFT technique. Square light regions: bare glass, pink lines: the blend on glass only.

vaporization methods and the LFT technique, which will be discussed below.

For LFT technique in this study, the PEDOT:PSS film is selected as the "layer-filter", i.e., the energy absorption and thermal decomposition are deliberately designed to occur only within this layer under the irradiation of the laser with 1064 nm wavelength. A confined pressure is thus constructed and the subsequent explosion effect is sufficient to purge away the upper layers. To demonstrate this strategy, a multilayer structure with P3HT:PC_{61}BM/PEDOT:PSS/glass is first designed, in which the P3HT:PC_{61}BM blend film was spin-coated on PEDOT:PSS layer with prescratched mesh pattern (Figure 1c). If this strategy is feasible, the regions covered with both PEDOT:PSS and P3HT:PC_{61}BM blend film should be removed under the NIR laser irradiation, while the P3HT:PC_{61}BM blend film contacting directly to the glass substrate would still remain. Figure 1d shows the optical microscopy (OM) picture of this structure after LFT ablation, which coincides well with our expectation. When irradiated by the NIR laser in a fully scanning coverage way with the laser fluence of 1.00 J cm^{-2}, all the film was cleared away with satisfactory resolution except the part in the scratched area thus forming the mesh pattern.

In addition, the different effect of the structure with and without PEDOT:PSS layer on the laser irradiation gives us a hint that if the pattern on the PEDOT:PSS layer is precisely predesigned according to requirements, one does not need to take the laser beam position into consideration for the subsequent LFT ablation. In other words, what you need to do is to irradiate the surface in a wide coverage, then the aimed pattern will be obtained by the "self-aligned" effect of the LFT technique. This effect is of great importance for the merged P1–P2 line processing (P1 line for the separation of bottom electrodes and P2 line for the exposure of the bottom electrode surface for its contact with the adjacent top electrode as a series connection), which will be discussed in details in the following section.

2.2. Determination of Laser Fluence in LFT Technique and Its Effect on Merged P1–P2 Line Design

As discussed above, the LFT technique is applicable for the fabrication of organic photovoltaic module devices from the viewpoint of the rationale. However, during the real operation, the process window related to the laser energy still needs to be finely adjusted to ensure that the PEDOT:PSS "filter-layer" is just completely ablated while the underlying layer is not affected. Therefore, the effect of the laser irradiation with the fluencies of 0.28–2.21 J cm^{-2} was investigated on the multilayer structure with the stacking sequence of P3HT:PC_{61}BM/PEDOT:PSS/ITO on glass substrate. **Figure 2**a shows the OM picture of the irradiated surface, in which the horizontal groove is only P3HT:PC_{61}BM on glass, and the corresponding surface profile is given in Figure 2b.

From Figure 2a, it can be seen that when the surface of the multilayer structure is irradiated with 2.21 J cm^{-2} of laser fluence, the PEDOT:PSS and P3HT:PC_{61}BM layers are completely removed (Figure $2a_1$). However, because 2.21 J/cm^2 is much higher than 1.10 J cm^{-2}, which is the ablation threshold for the bared ITO layer under the experimental condition (Table S1, Supporting Information), the overflow of the fluence inevitably damages the bottom ITO layer and remains the ring-like spot with diameter of 53 μm along the scanning channel on the glass substrate. The ring-like spot is suggested to be resulted from the Gaussian effect of the NIR laser beam, for which the energy decreases from the centre to the edge of the laser beam. The profile shown in Figure 2b gives the depths of 130 and 150 nm corresponding to the different scanning channels, which are in good agreement with the thicknesses of organic (PEDOT:PSS and blend) and ITO layers, respectively.

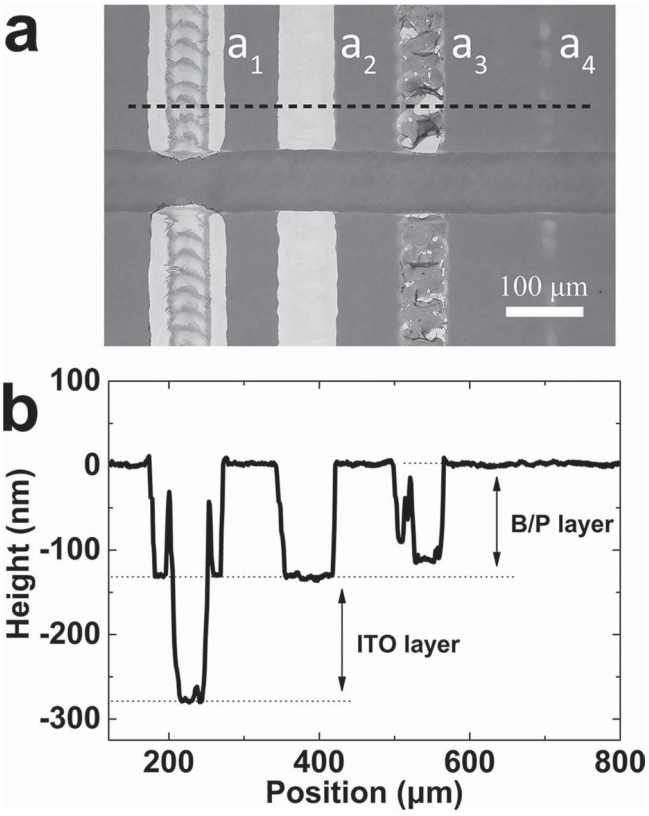

Figure 2. a) OM image of the surface of blend/PEDOT:PSS/ITO/glass structure irradiated with laser fluences of a_1) 2.21 J cm^{-2}, a_2) 1.00 J cm^{-2}, a_3) 0.53 J cm^{-2}, and a_4) 0.28 J cm^{-2}. The horizontal groove is P3HT:PC_{61}BM blend film on glass substrate. b) The corresponding surface profile.

When the laser fluence decreases to 1.00 J cm^{-2}, it is found that the PEDOT:PSS layer together with top blend layer is completely removed while no damaged traces are observed on the bottom ITO layer (Figure $2a_2$), which is also demonstrated by 130 nm of the depth shown in Figure 2b. For LFT technique, it is mentioned that the removal of the blend layer is reached by the explosive evaporation, which is initiated by the decomposition of the "layer-filter". This unique advantage avoids the utilization of high laser fluence and thus eliminates the occurrence of the edge bulge caused by the material carbonation. As shown in Figure 2, the smooth edge of the channel and instant change in the depth from the top surface to the ITO layer without fluctuation are obtained, which are especially beneficial for the precise design and control in the fabrication of the module device.

If the laser fluence further decreases to 0.53 J cm^{-2}, the decomposition of PEDOT:PSS layer could also take place.

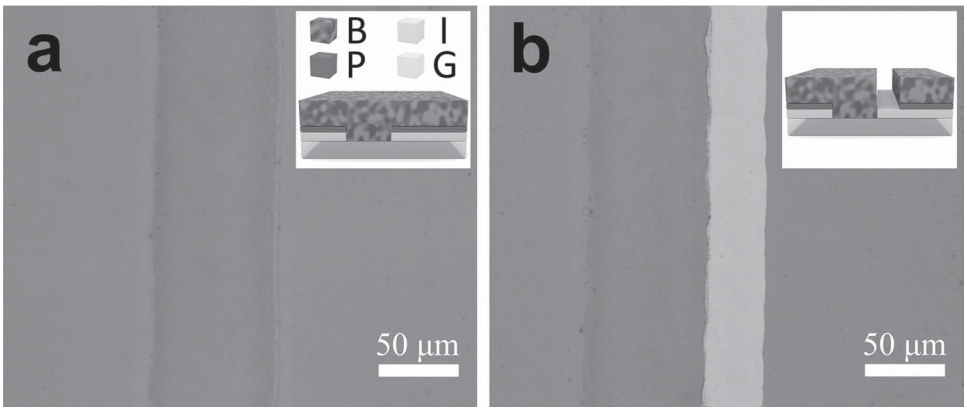

Figure 3. a) OM image of P1 line. b) The merged P1–P2 line design through LFT technique. The insets are the schematic illustrations of the film stacking order including the active material blend (B), PEDOT:PSS (P), ITO (I), and glass substrate (G).

However, the low fluence only initiates partial evaporation of the layer, which could not establish the effective confined pressure to purge away the blend film, thus the irregular film debris are still loosely attached to the irradiated surface (Figure 2a$_3$). Much lower laser fluence of 0.28 J cm^{-2} is also examined, and it is found that this dose does not bring any effects on the surface of the multilayer structure, but do degrade the blend film to some extent, as indicated by the regions with light colour shown in Figure 2a$_4$.

Again, the horizontal groove shown in Figure 2a, which is only the P3HT:PC$_{61}$BM blend film on glass substrate, does not exhibit any changes before and after irradiation, irrespective of the laser fluence ranging from 0.28 to 2.21 J cm^{-2}.

As demonstrated above, when the laser irradiation acts on surface, the multilayer structure with and without PEDOT:PSS layer-filter shows different ablation effects. As an inspired consequent, this "self-aligned" effect of the LFT technique is favorable for the merged P1–P2 line processing to erase the spacing between traditional P1 line and P2 line. **Figure 3** shows the pristine P1 line and the merged P1–P2 line after irradiation with 1.00 J cm^{-2} of laser fluence (irradiation center along the boundary line), from which it can be seen that the width of P1 line keeps unchanged while the P2 line is ablated to 35 μm of width. It could be imagined that as the degree of the overlapping between the irradiation area and the P1 line varies, the width of P2 line is adjustable. As shown in Figure S1 (Supporting Information), the widths of the P2 lines with 55 and 85 μm are achieved for lower and no overlapping degree, respectively. Therefore, the merged P1–P2 line design through the "self-aligned" ablation method clearly provide us with the flexibility in the trade-off between contact resistance and P2 line width, especially for the large area photovoltaic devices which require more elaborate designs to reduce the Joule heat loss at the connection portion between the single cells.

2.3. LFT Technique for Top Electrode Split

In CLA method, compared to polymer materials, much higher fluence or rigorous process window must be reached for the ablation of the top electrode, due to high boiling point of the metal and the reflectivity of the mirror surface in some cases.[29–32] For LFT technique, the removal of the metal electrode layer could also be readily implemented (**Figure 4**), but in contrast, only much lower fluence threshold is required through the smart regulation of the processing direction from the top to the bottom.

Figure 4a shows the surface of the stacking Al/Ca/blend/PEDOT:PSS/ITO/glass structure irradiated from the top according to CLA method. Since the metal electrode

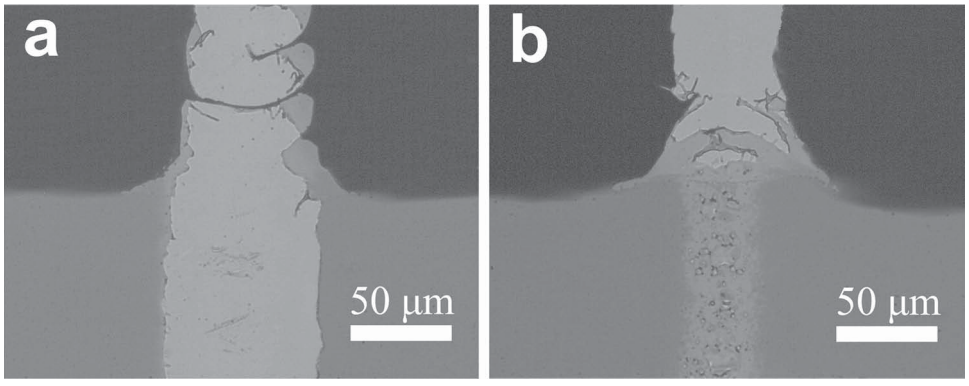

Figure 4. OM images of ablated electrode/blend/PEDOT:PSS/ITO/glass structure. a) Top irradiation with fluence of 1.18 J cm^{-2} (CLA method). b) Bottom irradiation with fluence of 0.28 J cm^{-2} (LFT technique).

possesses high boiling point and reflectivity, much higher laser fluence (1.18 J cm^{-2}) is needed for the complete separation of the electrode layer, which is higher than that for the P2 step in LFT technique (1.00 J cm^{-2}). From Figure 4a, it can be seen that although the conventional method could achieve the electrode ablation together with the removal of the blend and PEDOT:PSS sublayers, the traces of the remained electrode and the damaged ITO layer are clearly observed, and the scanning area without covered electrode layer broadens obviously. These could be ascribed to the incontinuous adjustment of the laser fluence during the processing, and in some cases, the fixed laser fluence is overflow due to the different sensitivity of the materials.

For LFT technique, however, to avoid the influence of the top electrode layer, the irradiation direction is smartly changed from the top to the bottom, i.e., laser irradiation from the bottom of the structure. As a consequence, much lower laser fluence (only 0.28 J cm^{-2}) is required due to the existence of the PEDOT:PSS "layer-filter". Figure 4b shows the OM image of the irradiated surface, from which it can be seen that the top electrode layer is completely removed. An interesting finding is that under this irradiation condition, the bare blend film without covered electrode layer is not removed away, and the scanning area with obvious damaged spots narrows to the width of ≈30 µm. This is the strong evidence of the LFT technique. In other words, the PEDOT:PSS "layer-filter" do decompose under the laser irradiation with 0.28 J cm^2 of fluence. The vaporization of the layer establishes a confined pressure, which subsequently exerts the explosion effect on the top layers. The layer consisting of electrode and blend is easily purged away by the explosion due to its rigid and fragile feature. While for the bare blend layer, because of its relatively high flexibility, the explosion process is not sufficient to completely remove the layer, which only results in damaged spots on the loosely attached film. Beside the "layer-filter", it should be mentioned that the much lower laser fluence for this step might also be related to the mirror reflectivity of the smooth metal electrode layer, which could accelerate the light absorption of the "layer-filter".

The presence of the PEDOT:PSS "layer-filter" is extremely important for the LFT technique. This could be seen from Figure S2 (Supporting Information), in which the multilayered structure with the stacking sequence of Al/Ca/P3HT:$PC_{61}BM$/ITO/glass was irradiated from bottom with the laser fluencies of 0.28 and 1.18 J cm^{-2}, respectively. The absence of the PEDOT:PSS "layer-filter" made the processing switched from the LFT technique to the conventional method. Consequently, the lower irradiation results in nothing but only few cracks on the surface (Figure S2a, Supporting Information), while the higher one leads to the irregular patterns formed by peeling the layers off the surface (Figure S2b, Supporting Information).

The advantages of the LFT technique over the CLA method for the electrode layer ablation are further clearly demonstrated by OM observation and surface profile measurement, as presented in **Figure 5**. After irradiation with 1.18 J cm^{-2} of laser fluence from top, the surface of the multilayer structure shows a thread of solid spots on the irradiated channel. This is caused by the Gaussian effect of the laser beam, which is also responsible for the ≈50 µm wide channel (smaller than ≈75 µm of the beam diameter), indicating the low efficiency

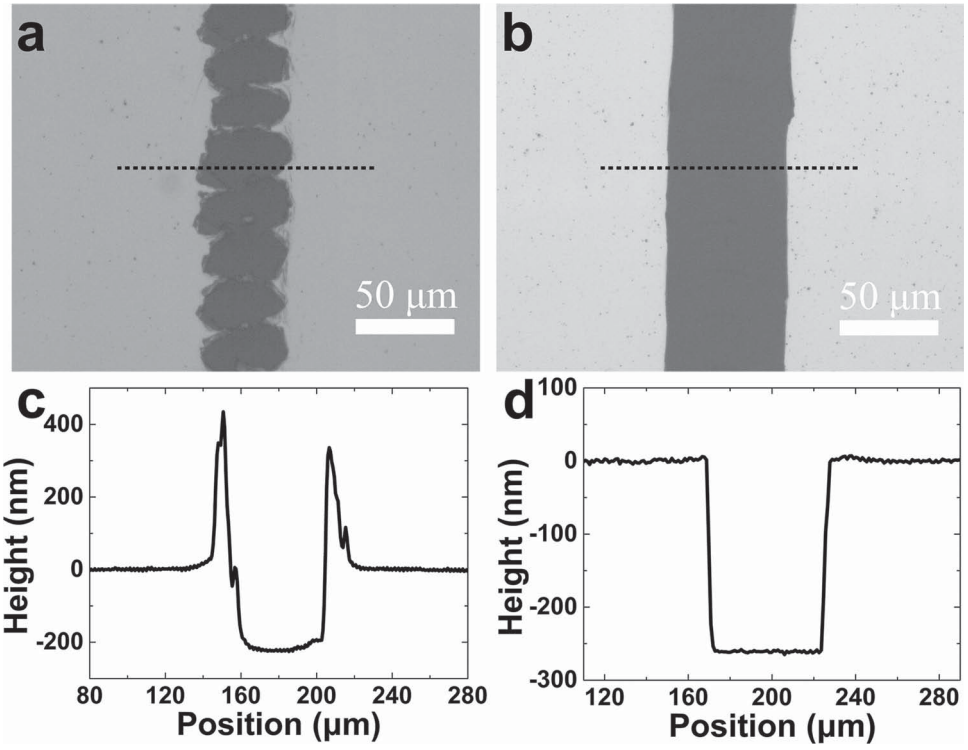

Figure 5. OM images and corresponding surface profiles of ablated electrode/blend/PEDOT:PSS/ITO/glass structure. a,c) Top irradiation with fluence of 1.18 J cm^{-2} (CLA method); b,d) bottom irradiation with fluence of 0.28 J cm^{-2} (LFT technique).

of energy utilization for CLA method. Figure 5a also shows the traces of the remaining electrode layer in the irradiated channel, which greatly increase the short-circuit risk of the device. In addition, the profile shown in Figure 5c manifests the peaks high up to ≈400 nm at the edge and the channel deep to only around 220 nm (260 nm if totally removed), revealing the low quality of the conventional ablation method in this study.

Totally different topography is obtained for the LFT technique with 0.28 J cm^{-2} of laser influence. From Figure 5b,d, it can be seen that the back irradiation forms uniform irradiated channel with around 60 μm of width and 260 nm of depth, which indicates the high efficiency of energy utilization and the complete removal of the PEDOT:PSS/blend/electrode layer. The explosive evaporation of the "layer-filter" under irradiation also results in smooth edges of the channel in terms of decreasing thermal damage.

2.4. LFT Technique for Photovoltaic Module Fabrication and Device Characteristics

Based on the step-by-step elucidation of the LFT technique, the photovoltaic modules with the cells in series with the normal layer sequence of Al/Ca/P3HT:$PC_{61}BM$/PEDOT:PSS/ITO as shown in **Figure 6**a are fabricated. Taking into account that ITO layer can be ablated with the 1064 nm wavelength NIR laser to satisfactory quality (P1 Step), all the pattern processes are achieved through the NIR laser with a single wavelength of 1064 nm as illustrated in Figure 6b–d. First, the PEDOT:PSS spin-coated ITO layer is ablated with fluence of 2.54 J cm^{-2} to separate the bottom electrodes of the adjacent single cells (Figure 6b, CLA method). Then P2 Step proceeds from the top irradiation with the fluence of 1.00 J cm^{-2} (Figure 6c, LFT technique). Finally, back irradiation with the fluence of 0.28 J cm^{-2} for P3 step is carried out (Figure 6d, LFT technique). Following the above procedure, the module device with five cells in series, in which the active area of 4 mm × 24 mm for single cell is connected with the dead area of 0.3 mm × 24 mm, is obtained, as shown in Figure 6e. The total active area of the module device is 4.8 cm^2, and its geometric fill factor (GFF) is calculated to be higher than 90%, which implies that the LFT technique shows a plenty of room for further improving the device GFF by increasing the width of the single cell to around 1.0–1.1 cm, which has been well recognized to be the optimum size for the module devices.[33]

It is worth to note that although the laser fluences used in the device fabrication are fixed for P1, P2, and P3 steps in this study; in fact, a range of the fluence could be applied. For example, the fluences for PEDOT:PSS "layer-filter" in the P2 and P3 steps could be in the range of 0.75–1.10 J cm^{-2} and 0.25–1.10 J cm^{-2}, respectively (Table S1, Supporting Information), indicating the wide process window of the LFT technique.

Figure 7 and **Table 1** show the current density–voltage (J–V) characteristics and corresponding values of the module device shown in Figure 6e, respectively. These parameters indicate that the open-circuit voltage (V_{oc}) strictly follows a linear growth (±2.1%) while the total short-circuit current (I_{sc}) is almost unchanged (±3.8%) with increasing the cell numbers in series. Combining with the steady variation (±2.8%) in fill factor (FF), the power conversion efficiency (PCE) of the module devices is consequently slightly decreased from 2.81% for single cell to 2.58% for five-cell series module device. In comparison to conventional infrared laser ablation methods, the precise quality and the processing stability obtained in this study by LFT technique, are first reported to reach so high level, to the best of our knowledge, which is even equivalent to that obtained by the ultrafast CLA methods with pulse duration of femtosecond or picosecond.[15,16,25,34]

2.5. Applicability of the LFT Technique

Based on the rationale, as long as the materials that used in the organic photovoltaic devices possess different sensitivity to the 1064 nm wavelength, the LFT technique could be applied. Considering that the conjugated polymers for solar cells generally possess an optical absorption edge below 1000 nm,[35–37] the module device based on low-bandgap polymer blend film is expected to could also be fabricated by the LFT technique. Here, the typical low-bandgap polymer, PBDT-TFQ, is selected. The absorption and thermal properties of PBDT-TFQ:$PC_{71}BM$ blend films are given in Figure S3 (Supporting Information), and the effect of the LFT technique on the device fabrication is exemplified by P3 step shown in Figure S4 (Supporting Information).

Following the same procedure (Figure 6) and the parameters listed in Table S1 (Supporting Information), the module device with the same size based on the stack structure of Al/Ca/PBDT-TFQ:$PC_{71}BM$/PEDOT:PSS/ITO is fabricated. The picture and characteristics of the device are shown in **Figure 8** (detailed values are given in Table S2 in the Supporting Information). Similarly, the linear growth in V_{oc} (±2.4%) together with the stabilities in I_{sc} (±8%) and FF(±0.7%) maintains the PCE at 4.27% for five-cell series module device (4.78% for single cell), which indicates the compatibility of the LFT technique for the low-bandgap material systems. It is noteworthy that both the PBDT-TFQ:$PC_{71}BM$ based and the P3HT:$PC_{61}BM$ based devices are fabricated with exactly the same set of ablation parameters, which implies the possibility of sharing parameters for different blend systems with the same "layer-filter" selected. In view of the dominance of the "layer-filter" in determining the processing window, the LFT technique would be easily performed as a general methodology.

3. Conclusion

In summary, a novel strategy, which is based on 1064 nm wavelength of the NIR laser and named as LFT technique, is developed and demonstrated in this study for the patterning processing of multilayer organic semiconductor devices. For the typical stack structure in PSCs as metal/blend/PEDOT:PSS/ITO/glass, with this new technique, the PEDOT:PSS serves as the "layer-filter", whose decomposition under irradiation constructs a confined pressure and thus purges away the upper layers by subsequent explosive

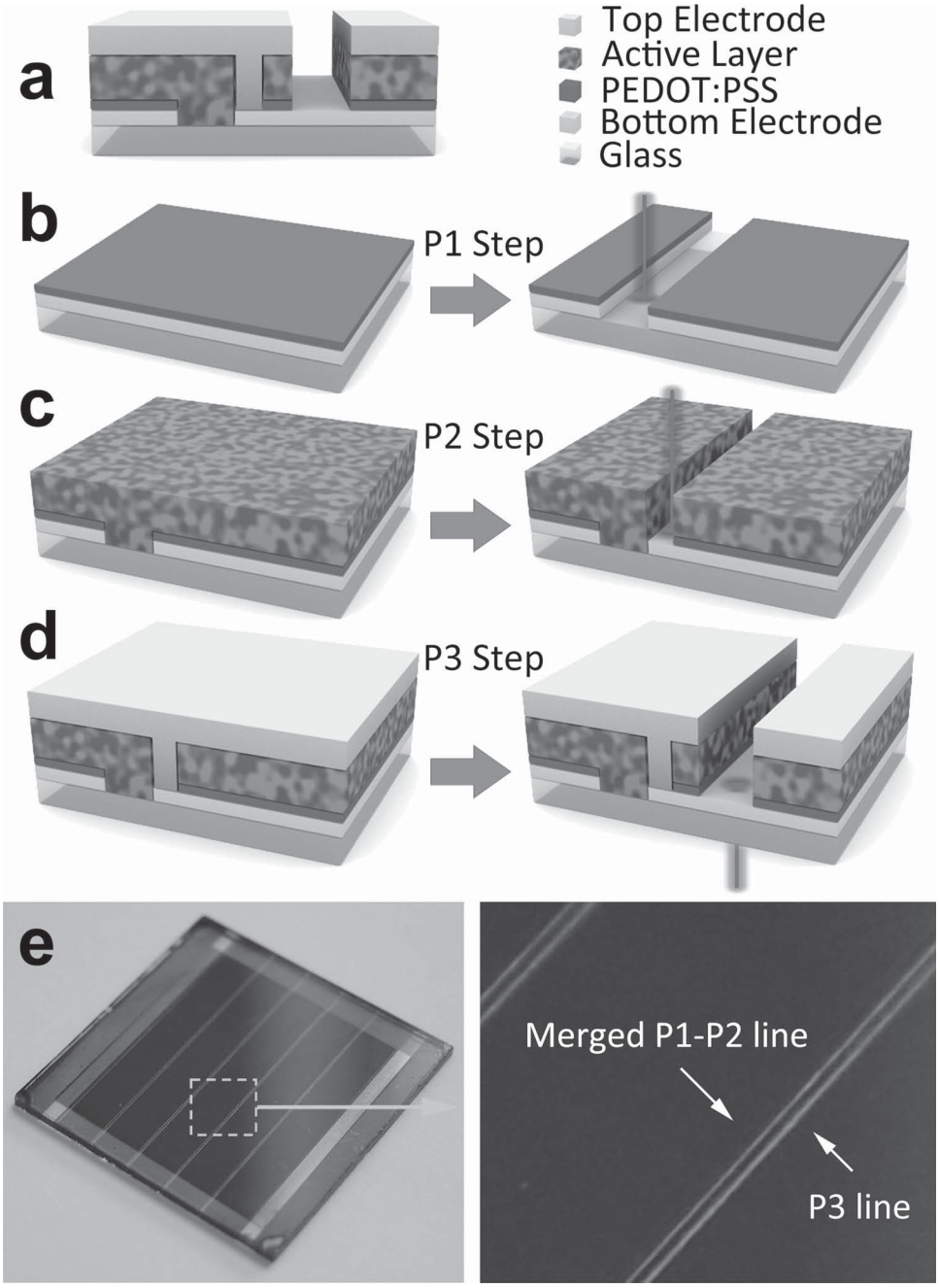

Figure 6. a) Schematic illustration of the device configuration and b–d) LFT procedures for photovoltaic module fabrication. e) The photographic image of a sample module device based on P3HT:$PC_{61}BM$ through the LFT method.

evaporation effect. This unique principle involves only low energy threshold, and the "self-aligned" feature through a patterned "layer-filter" has been demonstrated, with which the merged P1–P2 line design is realized for a further reduction of the dead areas. The patterning of the metal electrode layer could also be readily achieved by changing the processing direction. Module devices based on the classical P3HT:$PC_{61}BM$ system and the low-bandgap PBDT-TFQ:$PC_{71}BM$ system with 4.8 cm^2 of total active area, in which five single cells with individual active area of 4 mm × 24 mm are connected with the dead area of 0.3 mm × 24 mm, are successively fabricated by LFT technique. It is found that this new technique shows excellent processing accuracy and over 90% of GFF is reached, which is accompanied by the stable device performance (PCE, I_{sc}, V_{oc}, and FF) with the increased number of cells in series. In comparison to CLA methods, the LFT technique proposed in this study uses the industry available laser sources and reaches the comparable processing precision, which is proved to be a promising way in the manufacture of organic semiconductor devices.

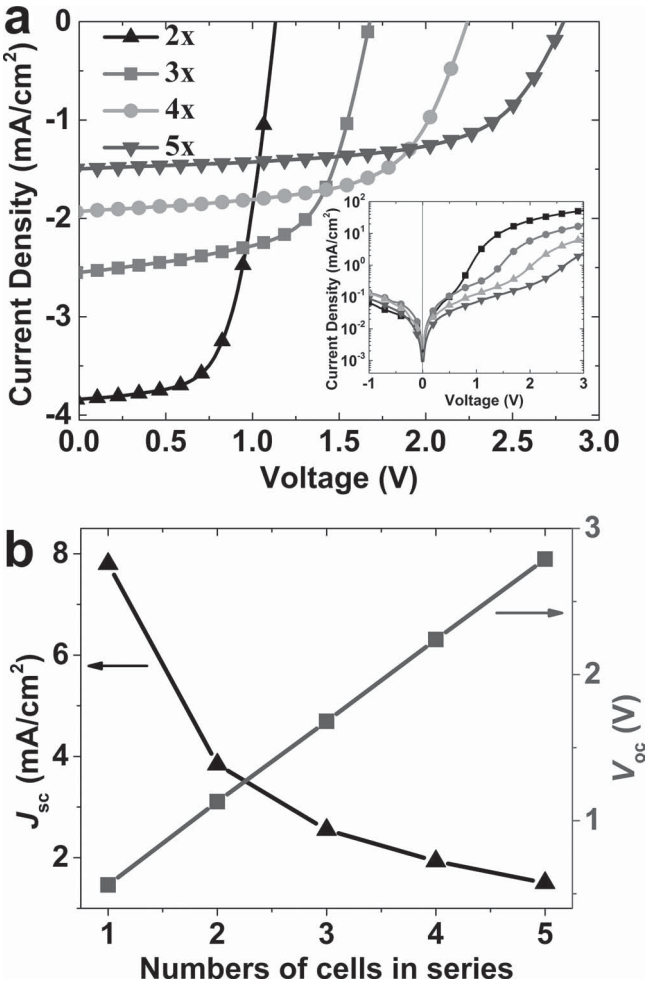

Figure 7. a) *J–V* characteristics of LFT technique fabricated module device based on P3HT:$PC_{61}BM$ blend film. The inset is the *J–V* character measured under dark condition. b) Variations in short circuit current (J_{sc}) and open circuit voltage (V_{oc}) with the number of the cells in series of the modules based on P3HT:$PC_{61}BM$ blend film.

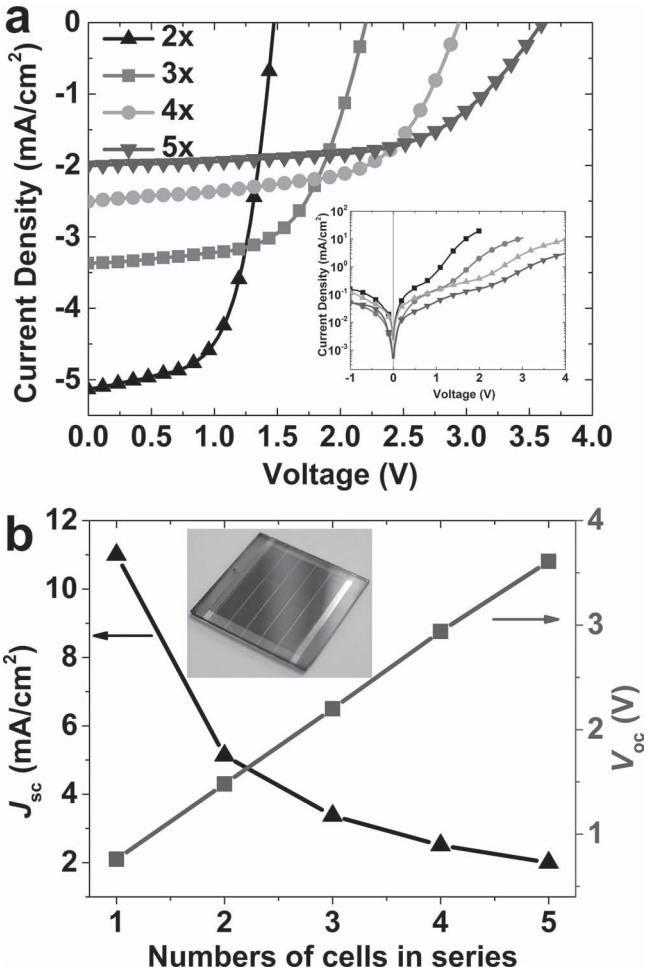

Figure 8. a) *J–V* characteristics of the module device based on PBDT-TFQ:$PC_{71}BM$, the inset is the *J–V* character measured under dark condition. b) Variations in short circuit current (J_{sc}) and open circuit voltage (V_{oc}) with the number of the cells in series of the modules based on PBDT-TFQ:$PC_{71}BM$ blend film, inset is picture of the module device.

4. Experimental Section

Materials: P3HT (M_n = 47 kg mol^{-1}, PDI = 1.72) and PBDT-TFQ (M_n = 35 kg mol^{-1}, PDI = 2.0) were synthesized according to the previous literatures.[38,39] *O*-dichlorobenzene (ODCB, anhydrous, 99%) and poly(3,4-ethylenedioxythiophene): poly(styrene sulfonate) (PEDOT:PSS) Al4083 were purchased from Sigma-Aldrich and H.C. Starck GmbH, respectively. $PC_{61}BM$ (99.5%) and $PC_{71}BM$ (99.0%) were obtained from American Dye Source Inc. All these materials were used as received.

Laser Pattern Processing: For the laser ablation steps, a EP30-1 diode-end-pumped Nd:YVO4 laser (Changchun New Industries Optoelectronics Technology Co. Ltd.) was used, operating at 1064 nm of wavelength, 20 kHz of pulse repetition rate, and 8 ns of pulse duration (full width at half maximum). All the ablation steps were achieved with spot overlap of 50% with scanning speed of 500 mm s^{-1}, and the different input currents from the power module were adjusted to achieve corresponding laser fluences for different steps.

Fabrication of Photovoltaic Modules: Indium tin oxide (ITO)-coated glass with sheet resistance of 10 Ω square^{-1} was cleaned in ultrasonic bath with deionized water, acetone, and isopropanol alcohol for 20 min each and dried in a flow of nitrogen. The precleaned substrates were treated in UV-ozone for 20 min after which a 30 nm thick PEDOT:PSS layer was spin-coated followed by a 20 min baking treatment at 150 °C in atmosphere. Then the P1 line was ablated with laser fluence of 2.54 J cm^{-2} to form a unified pattern for both the PEDOT:PSS layer and ITO layer (P1 step). After that, a 100 nm thick P3HT:$PC_{61}BM$ (1:1, w/w) blend layer or 90 nm thick PBDT-TFQ:$PC_{71}BM$ (1:1, w/w) blend layer was spin-casted followed by a 10 min annealing treatment at 150 °C in glovebox. Then the organic layers were ablated by partially overlap method along the edge of P1 line with laser fluence of 1.00 J cm^{-2} to

Table 1. Photovoltaic properties of the P3HT:$PC_{61}BM$ module device.

Numbers of cells in series	V_{oc} [V]	J_{sc} [mA cm^{-2}]	FF [%]	PCE [%]	R_s [Ω cm^{-2}][a)]
1	0.57	7.80	63.10	2.81	10.10
2	1.13	3.84	62.03	2.68	9.89
3	1.68	2.55	61.36	2.63	10.15
4	2.24	1.93	61.64	2.66	10.55
5	2.79	1.50	61.79	2.58	10.67

[a)]Series resistances (R_s) were obtained from the *J–V* characteristics under dark condition.

maintain the merged P1–P2 line (P2 step). The top electrode was prepared with a 30 nm thick calcium layer followed by a 100 nm aluminum electrode layer deposited under vacuum of ca. 5×10^{-4} Pa and was separated using the back incident method under the fluence of 0.28 J cm^{-2} (P3 step) to complete the series structure of the modules. Detailed parameters of LFT technique used in the device fabrication were given in Table S1 (Supporting Information).

Characterization: Thermogravimetric analysis was carried out by TGA (Mettler-Toledo TGA/DSC 1) instrument in nitrogen atmosphere with a heating rate of 10 K min^{-1}. UV–vis–NIR absorption spectra were recorded on a Lambda 750 spectrometer (Perkin-Elmer, Wellesley, MA). OM images were taken with a Carl Zeiss A1m microscope. Film thicknesses were acquired by a KLA-Tencor D-100 surface profiler. Laser intensity was measured with LP-3C power meter (Physcience Opto-Electronics, Beijing). *J–V* characteristic measurements were performed in nitrogen atmosphere using a computer-controlled source-measure-unit (Keithley 2400) in the glovebox in the dark and under illumination with AM1.5G simulated solar light at intensity of 100 mW cm^{-2} generated from a 300 W xenon light source (XES-70S1, San-Ei Electric Co. Ltd., Osaka, Japan).

Supporting Information

Supporting Information is available from the Wiley Online Library or from the author.

Acknowledgements

This work was financially supported by the National Natural Science Foundation of China (Grant Nos. 20925415 and 20990233), the Solar Energy Initiative (Grant No. KGCX2-YW-399 + 9) of the Chinese Academy of Sciences and the Hi-Tech Research and Development Program (863) of China (Grant No. 2011AA050524).

Received: April 27, 2015
Revised: May 19, 2015
Published online: June 10, 2015

[1] N. Espinosa, M. Hösel, M. Jørgensen, F. C. Krebs, *Energy Environ. Sci.* **2014**, *7*, 855.
[2] R. R. Sondergaard, N. Espinosa, M. Jorgensen, F. C. Krebs, *Energy Environ. Sci.* **2014**, *7*, 1006.
[3] C. Duan, W. Cai, B. B. Y. Hsu, C. Zhong, K. Zhang, C. Liu, Z. Hu, F. Huang, G. C. Bazan, A. J. Heeger, Y. Cao, *Energy Environ. Sci.* **2013**, *6*, 3022.
[4] M. K. Siddiki, J. Li, D. Galipeau, Q. Qiao, *Energy Environ. Sci.* **2010**, *3*, 867.
[5] G. Li, R. Zhu, Y. Yang, *Nat. Photonics* **2012**, *6*, 153.
[6] Y. Michael Yang, W. Chen, L. Dou, W.-H. Chang, H.-S. Duan, B. Bob, G. Li, Y. Yang, *Nat. Photonics* **2015**, *9*, 190.
[7] L. Dou, J. You, Z. Hong, Z. Xu, G. Li, R. A. Street, Y. Yang, *Adv. Mater.* **2013**, *25*, 6642.
[8] J. Lee, H. Back, J. Kong, H. Kang, S. Song, H. Suh, S.-O. Kang, K. Lee, *Energy Environ. Sci.* **2013**, *6*, 1152.
[9] H. Kang, S. Hong, H. Back, K. Lee, *Adv. Mater.* **2014**, *26*, 1602.
[10] H. Kim, S. Lee, D. Han, S. Yoo, *Sol. Energy Mater. Sol. Cells* **2014**, *120*, 561.
[11] M. Kim, J. H. Park, J. H. Kim, J. H. Sung, S. B. Jo, M.-H. Jo, K. Cho, *Adv. Energy Mater.* **2015**, *5*, 1401317.
[12] R. Søndergaard, M. Hösel, D. Angmo, T. T. Larsen-Olsen, F. C. Krebs, *Mater. Today* **2012**, *15*, 36.
[13] C. J. Brabec, J. R. Durrant, *MRS Bull.* **2008**, *33*, 670.
[14] M. M. Voigt, A. Guite, D.-Y. Chung, R. U. A. Khan, A. J. Campbell, D. D. C. Bradley, F. Meng, J. H. G. Steinke, S. Tierney, I. McCulloch, H. Penxten, L. Lutsen, O. Douheret, J. Manca, U. Brokmann, K. Sönnichsen, D. Hülsenberg, W. Bock, C. Barron, N. Blanckaert, S. Springer, J. Grupp, A. Mosley, *Adv. Funct. Mater.* **2010**, *20*, 239.
[15] G. D. Spyropoulos, P. Kubis, N. Li, D. Baran, L. Lucera, M. Salvador, T. Ameri, M. M. Voigt, F. C. Krebs, C. J. Brabec, *Energy Environ. Sci.* **2014**, *7*, 3284.
[16] P. Kubis, N. Li, T. Stubhan, F. Machui, G. J. Matt, M. M. Voigt, C. J. Brabec, *Prog. Photovoltaics Res. Appl.* **2013**, *23*, 238.
[17] T. Blaudeck, P. A. Ersman, M. Sandberg, S. Heinz, A. Laiho, J. Liu, I. Engquist, M. Berggren, R. R. Baumann, *Adv. Funct. Mater.* **2012**, *22*, 2939.
[18] T. Lippert, *Plasma Process. Polym.* **2005**, *2*, 525.
[19] H. Jeon, R. Schmidt, J. E. Barton, D. J. Hwang, L. J. Gamble, D. G. Castner, C. P. Grigoropoulos, K. E. Healy, *J. Am. Chem. Soc.* **2011**, *133*, 6138.
[20] N. Bityurin, A. Malyshev, *J. Appl. Phys.* **2002**, *92*, 605.
[21] R. R. Gattass, E. Mazur, *Nat. Photonics* **2008**, *2*, 219.
[22] L. G. Reyna, J. R. Soběhart, *J. Appl. Phys.* **1995**, *78*, 3423.
[23] H. Schmidt, J. Ihlemann, B. Wolff-Rottke, K. Luther, J. Troe, *J. Appl. Phys.* **1998**, *83*, 5458.
[24] N. Bityurin, E. Arenholz, N. Arnold, D. Bäuerle, *Phys. Rev. E* **2007**, *75*, 1.
[25] P. Kubis, L. Lucera, F. Machui, G. Spyropoulos, J. Cordero, A. Frey, J. Kaschta, M. M. Voigt, G. J. Matt, E. Zeira, C. J. Brabec, *Org. Electron.* **2014**, *15*, 2256.
[26] N. Li, P. Kubis, K. Forberich, T. Ameri, F. C. Krebs, C. J. Brabec, *Sol. Energy Mater. Sol. Cells* **2014**, *120*, 701.
[27] J. Haenel, B. Keiper, C. Scholz, M. Clair, *Proc. SPIE 7771, Thin Film Solar Technology II* **2010**, *7711*, 77710G.
[28] T. Petsch, J. Haenel, M. Clair, B. Keiper, C. Scholz, *Proc. SPIE 7921, Laser-based Micro- and Nanopackaging and Assembly V* **2011**, *7921*, 79210U.
[29] J. Yang, Y. Zhao, N. Zhang, Y. Liang, M. Wang, *Phys. Rev. B: Condens. Matter Mater. Phys.* **2007**, *76*, 165430.
[30] O. Benavides, L. de la Cruz May, A. Flores Gil, *Opt. Express* **2013**, *21*, 13068.
[31] M. Domke, S. Rapp, H. Huber, *Phys. Procedia* **2012**, *39*, 717.
[32] G. Heise, M. Domke, J. Konrad, S. Sarrach, J. Sotrop, H. P. Huber, *J. Phys. D. Appl. Phys.* **2012**, *45*, 315303.
[33] H. K. Lyu, J. H. Sim, S. H. Woo, K. P. Kim, J. K. Shin, Y. S. Han, *Sol. Energy Mater. Sol. Cells* **2011**, *95*, 2380.
[34] F. Guo, P. Kubis, T. Przybilla, E. Spiecker, A. Hollmann, S. Langner, K. Forberich, C. J. Brabec, *Adv. Energy Mater.* **2015**, DOI: 10.1002/aenm.201401779.
[35] M. C. C. Scharber, D. Mühlbacher, M. Koppe, P. Denk, C. Waldauf, a. J. Heeger, C. J. J. Brabec, a. J. Heeger, *Adv. Mater.* **2006**, *18*, 789.
[36] N. Li, D. Baran, G. D. Spyropoulos, H. Zhang, S. Berny, M. Turbiez, T. Ameri, F. C. Krebs, C. J. Brabec, *Adv. Energy Mater.* **2014**, *4*, 1400084.
[37] E. Bundgaard, F. Livi, O. Hagemann, J. E. Carlé, M. Helgesen, I. M. Heckler, N. K. Zawacka, D. Angmo, T. T. Larsen-Olsen, G. a. dos Reis Benatto, B. Roth, M. V. Madsen, M. R. Andersson, M. Jørgensen, R. R. Søndergaard, F. C. Krebs, *Adv. Energy Mater.* **2015**, *5*, 1402186.
[38] R. S. Loewe, S. M. Khersonsky, R. D. McCullough, *Adv. Mater.* **1999**, *11*, 250.
[39] H. C. Chen, Y. H. Chen, C. C. Liu, Y. Chien, S. W. Chou, P. T. Chou, *Chem. Mater.* **2012**, *24*, 4766.